Int. J. Solids Structures Vol. 14, pp. 1027–1043

0020-7683/78/1201-1043/$02.00/0

INFLUENCE OF GEOMETRICAL PARAMETERS ON THE MODE OF COLLAPSE OF A "PINCHED" RIGID-PLASTIC CYLINDRICAL SHELL

S. R. REID

University Engineering Department, Cambridge, England

(*Received* 15 *March* 1978; *in revised form* 12 *July* 1978)

Abstract—The modes of collapse of a rigid-plastic circular cylindrical shell subjected to centrally applied, opposed point loads in which the deformation is not confined to the vicinity of the loaded points are analysed. It is shown that the solution is analogous to that of an equivalent beam-foundation problem and the analogy is discussed. The results are compared with observations made during a series of experiments concerned with the crushing of aluminium tubes by opposed indenters.

NOTATION

D diameter of cylinder
$\dot{\mathscr{D}}$ rate of dissipation of energy in plastic work
L half-length of beam or cylinder
M_p fully plastic moment of beam
M_0, N_0 fully plastic bending moment and membrane force per unit length for rigid–plastic cylinder
M_1, M_2, M_{12} bending and twisting unit moments acting on shell element
$M_x, M_\theta, M_{x\theta}$ axial, circumferential unit bending and twisting moments for circular cylindrical shell
N_1, N_2, N_{12} membrane direct and shear forces per unit length acting on shell element
N_x, N_θ axial and circumferential unit forces for circular cylindrical shell
P applied force
P_A collapse load per unit length for circular cylinder under ring load
P_B collapse load for rigid-plastic beam-foundation system
P_C collapse load for "pinched" cylinder
P_L collapse load for localised collapse mode (Fig. 2d)
P_O collapse load for reversed ovality mode (Fig. 2c)
P_R collapse load for ring mode (Fig. 2b)
P_1, P_2, P_3 collapse loads for centrally loaded beam on rigid-plastic foundation corresponding to modes shown in Fig. 4(b, c and d)
P_I, P_{II}, P_{III} collapse loads for ring-loaded cylinder corresponding to modes shown in Fig. 5(b, c and d)
R, T radius and wall-thickness of ring-loaded cylinder.
S area of region idealised by generalised plastic hinge (Fig. 1)
b constant occurring in eqn (9) *et seq* equal to 0.106
c constant occurring in eqn (9) *et seq* equal to 0.414
h width of region idealised by generalised plastic hinge (Fig. 1)
l length of generalised plastic hinge (Fig. 1)
p_0 rigid-plastic foundation yield pressure
r, t radius and wall-thickness of "pinched" cylinder
s, s^* half width of localised zone of collapse for "pinched" cylinder (Fig. 2d) and its optimum value
s_A, s_A^* half-width of localised zone of collapse for ring-loaded cylinder (Fig. 5d) and its optimum value
s_B, s_B^* half-width of localised zone of collapse for rigid plastic beam-foundation system (Fig. 4d) and its optimum value
$u_i = (u, v, w)$ displacement components
α, α^* normalised slope of top generator of "pinched" cylinder and its optimum value for reversed ovality (Fig. 2c)
β inclination of generalised plastic hinge to coordinate directions η_i (Fig. 1)
δ load-deflection for crushed tubes
$\dot{\epsilon}_1, \dot{\epsilon}_2, \dot{\gamma}_0$ membrane strain rates for shell element
θ polar coordinate
$\dot{\kappa}_1, \dot{\kappa}_2, \dot{\kappa}_{12}$ curvature and twist rates for shell element
η_i coordinate directions for analysis of generalised hinge (Fig. 1)
Ω angular velocity of edges of cylindrical shell panels (see Appendix)
Ω_1, Ω_2 components of relative rotation rates between regions A and B (Fig. 1) along the η_1 and η_2 axes respectively
Ω_x, Ω_θ relative rotation rates between conterminous zones in cylindrical shell

INTRODUCTION

The collapse of a rigid-plastic cylindrical shell under the influence of an axisymmetric ring load has been examined by a number of authors [1–3]. The problem consists basically of an

interaction between axial bending and circumferential stretching deformations of the shell wall. These deformation modes and the geometry of the shell determine the collapse load and the mechanism of collapse. The complexity of the solution depends to a large extent on the particular yield surface used. The limited interaction yield surface in which the onset of yield for membrane and bending deformations are determined independently (see Fig. 3) provides the simplest solution.

Using this simple yield surface an interesting analogy emerges between this axisymmetric shell problem and that of a rigid-plastic beam resting on a rigid-plastic Winkler foundation with a concentrated load applied at a point along its length. In the analogy the yield moment of the beam corresponds to the axial bending of the shell and the yield pressure of the foundation to the circumferential stretching of the shell. Whilst it would appear that this analogy has not been stated explicitly in the literature, its implicit use is clear in certain limit analyses involving cylindrical shell components such as that found in the paper by Dinno and Gill[4].

The analogy between the behaviour of a cylinder under axisymmetric loading and a beam-foundation interaction is well known in elastic shell theory[5]. Recently the analogy has been extended by Calladine[6] to provide approximate solutions to problems involving non-axisymmetric loading of elastic spherical and cylindrical shells. In particular, the problem of a "pinched" cylinder (i.e. a cylinder subjected to a pair of diametrically opposed, radially inward, point loads applied at its centre) was treated in some detail. By using simplified deformation fields which satisfy the compatibility requirements, Calladine showed that for a long cylinder the load was carried principally by an interaction between axial stretching and circumferential bending of the shell wall. Retaining only the contributions to the elastic strain energy arising from these two components of the deformation, the analogy with an equivalent beam-foundation system became apparent. The flexural rigidity of the beam derives from the axial stretching of the shell and the foundation stiffness from the circumferential bending.

The analysis contained in this paper can be considered to be a formal attempt to extend the analogy for the "pinched" cylinder problem into the realm of rigid-perfect plasticity. However, consideration of the title problem arose mainly out of an interest in explaining certain features of the behaviour of metal tubes when they are crushed between opposed indenters. This problem has been surveyed experimentally by Watson *et al.*[7]. The work described in [7] was principally concerned with the use of metal tubes as components of impact energy absorbing systems. The use of simple metal structures and structural elements for this purpose leads to a consideration of a number of interesting structural plasticity problems some of which have recently been reviewed[8].

One of the basic features of the mode of deformation of tubes when they are crushed is that the cross section of all or of a considerable portion of the tube undergoes plastic ovalisation. It is clear from [7] that a complete analysis of the tube crushing problem would be most complex. However, a preliminary attempt is made below to investigate the influence of the geometrical parameters on the mode of deformation by constructing a simple upper bound solution to the problem. This is based on the assumption that ovalisation is a prime component in the deformation mode for tubes of all lengths. It will be shown that the solution produced has many of the features that one might expect from Calladine's solution of the elastic problem. In particular, a beam-foundation analogy is established which could be of use in the solution of related problems.

In order to compare this upper bound solution with the behaviour of crushed tubes, the relevant experimental observations are summarised and the question of the usefulness of the analysis is discussed.

LIMIT ANALYSIS OF "PINCHED" CYLINDER

The mode of collapse of the cylinder is considered to be composed of a number of inextensional regions separated by plastic hinges. The loading is not axisymmetric and consequently neither is the velocity field which describes the incipient motion of the shell. This has the effect that within certain of the plastic hinges there is plastic membrane action as well as bending deformation. For this reason the discontinuity is termed a generalised hinge and its treatment follows that given by Jones and Walters[9].

Generalised plastic hinges

Figure 1 shows a plan view of a segment of a plastic region of width h and length l separating two regions A and B. From [9], the rate at which energy is dissipated in plastic work within this region, $\dot{\mathscr{D}}$, is given by

$$\dot{\mathscr{D}} = \int_S (N_1\dot{\epsilon}_1 + N_2\dot{\epsilon}_2 + N_{12}\dot{\gamma}_0 + M_1\dot{\kappa}_1 + M_2\dot{\kappa}_2 + 2M_{12}\dot{\kappa}_{12})\,\mathrm{d}S. \tag{1}$$

The symbols used for the generalised stress resultants and deformation rates have their usual meanings and are defined in the notation. S is the area of the deforming region. Suppose that $\dot{u}_i$ are the displacement rates in the η_i directions and Ω_i are the components along the η_i axes of the relative rotation rates between regions A and B. If we assume that the displacement rates vary linearly across the deforming region then the strain rates can be defined as

$$\dot{\epsilon}_1 = \frac{[\dot{u}_1]\sin\beta}{h}, \quad \dot{\epsilon}_2 = \frac{[\dot{u}_2]\cos\beta}{h} \text{ and } \dot{\gamma}_0 = \frac{[\dot{u}_1]\cos\beta + [\dot{u}_2]\sin\beta}{h}$$

where [ ] represents the difference between the values of the enclosed parameter in region B and in region A. Similarly the curvature rates are

$$\dot{\kappa}_1 = \frac{\Omega_1\sin\beta}{h}, \quad \dot{\kappa}_2 = \frac{\Omega_2\cos\beta}{h} \text{ and } 2\dot{\kappa}_{12} = \frac{\Omega_1\cos\beta + \Omega_2\sin\beta}{h}.$$

Since $\mathrm{d}S = h\,\mathrm{d}l$, we can proceed to the limit of a line of discontinuity ($h \to 0$). Equation (1) reduces to

$$\dot{\mathscr{D}} = \int_l \{N_1[\dot{u}_1]\sin\beta + N_2[\dot{u}_2]\cos\beta + N_{12}[\dot{u}_1]\cos\beta + N_{12}[\dot{u}_2]\sin\beta$$
$$+ M_2\dot{\kappa}_1 + M_1\Omega_1\sin\beta + M_2\Omega_2\cos\beta + M_{12}\Omega_1\cos\beta + M_{12}\Omega_2\sin\beta\}\,\mathrm{d}l. \tag{2}$$

Velocity fields

The circular cylinder of radius r, wall thickness t and length $2L$ is loaded as shown in Fig. 2(a). It is assumed that each half of the cylinder has an incipient collapse mode which consists in general of four panels I–IV which undergo inextensional deformation and a rigid end region V, the various regions being separated by plastic hinges. Clearly if the deforming region extends to the ends of the tube, region V does not exist.

Let us now define the velocity field associated with region I. It is shown in the Appendix that the conditions of inextensibility together with the simple velocity field for a ring subjected

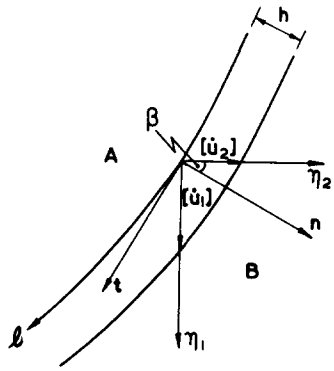

Fig. 1. Plan view of segment of plastic hinge connecting regions A and B from Ref. [8].

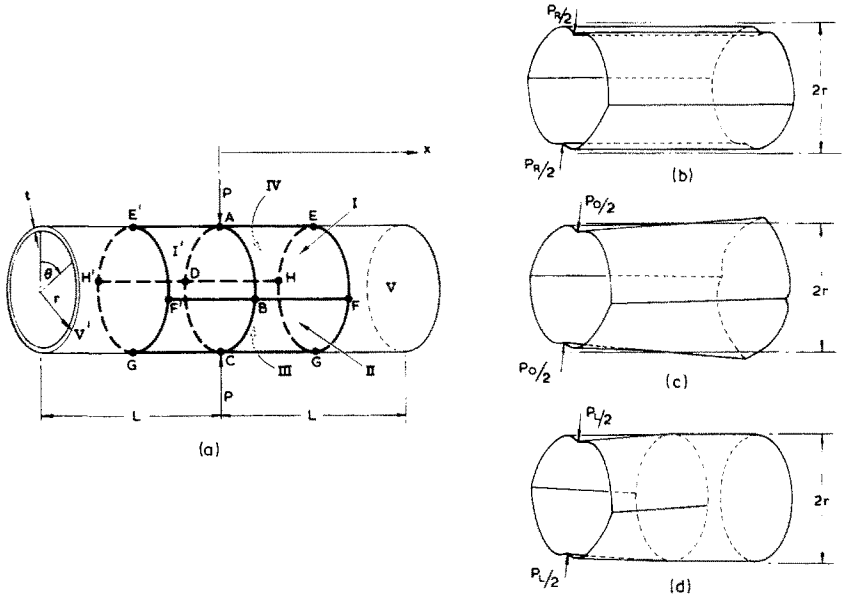

Fig. 2. (a) Hinge system for general mode of collapse of rigid-plastic "pinched" cylinder. (b) Ring mode for half of "pinched" cylinder. (c) Reversed ovality mode for half of "pinched" cylinder. (d) Localised mode for half of "pinched" cylinder.

to the same system of loads leads to the following:

In region I, $x > 0$ and $0 < \theta < \pi/2$

$$\dot{u} = \alpha r^2 \Omega \left(\frac{\pi}{4} - \theta + \sin\theta - \cos\theta \right).$$

$$\dot{v} = (1 - \alpha x) r\Omega (\sin\theta + \cos\theta - 1)$$

$$\dot{w} = -(1 - \alpha x) r\Omega (\cos\theta - \sin\theta) \tag{3}$$

where u, v and w are the axial, tangential and radial displacements, Ω is the angular velocity of the edge AB and α is the normalised slope of the (part) generator AE.

Whilst the velocity field defined by eqns (3) is inextensional, if $\alpha \neq 0$ the panel undergoes twisting deformation. Since[6]

$$\dot{\kappa}_x = -\frac{\partial^2 \dot{w}}{\partial x^2}, \quad \dot{\kappa}_\theta = -\frac{1}{r^2}\frac{\partial^2 \dot{w}}{\partial \theta^2} + \frac{1}{r^2}\frac{\partial \dot{v}}{\partial \theta}$$

and

$$\dot{\kappa}_{x\theta} = -\frac{1}{r}\frac{\partial^2 \dot{w}}{\partial x \partial \theta} + \frac{3}{4r}\frac{\partial \dot{v}}{\partial x} - \frac{1}{4r^2}\frac{\partial \dot{u}}{\partial \theta} \tag{4}$$

we have

$$\dot{\kappa}_x = \dot{\kappa}_\theta = 0 \text{ and } \dot{\kappa}_{x\theta} = \alpha\Omega \tag{5}$$

within region I.

Using simple symmetry arguments, the velocity fields in region IV and in the panel region separated from I by AB, i.e. region I', can be deduced from eqn (3).

In region I', $x < 0$ and $0 < \theta < \pi/2$

$$\dot{u} = -\alpha r^2 \Omega \left(\frac{\pi}{4} - \theta + \sin\theta - \cos\theta \right)$$

$$\dot{v} = (1 + \alpha x) r\Omega (\sin\theta + \cos\theta - 1)$$

$$\dot{w} = -(1 + \alpha x) r\Omega (\cos\theta - \sin\theta). \tag{6}$$

In region IV, $x > 0$ and $-\pi/2 < \theta < 0$

$$\dot{u} = \alpha r^2 \Omega \left(\frac{\pi}{4} + \theta - \sin\theta - \cos\theta\right)$$

$$\dot{v} = (1 - \alpha x)\, r\Omega\, (\sin\theta - \cos\theta + 1)$$

$$\dot{w} = -(1 - \alpha x)\, r\Omega\, (\cos\theta + \sin\theta). \tag{7}$$

For cylindrical shells it can also be shown [9] that the relative rotation rates between adjacent zones are given by

$$\Omega_x = -\left[\frac{\partial \dot{w}}{\partial x}\right] \text{ and } \Omega_\theta = \frac{[\dot{v}] - \left[\frac{\partial \dot{w}}{\partial \theta}\right]}{r}. \tag{8}$$

Analysis of various collapse mechanisms

Proceeding in the usual manner for constructing upper bound solutions in limit analysis, we consider various competing collapse mechanisms and then determine the range of applicability of each. It can be shown that there are three competing mechanisms and these are shown in Figs. 2(b, c and d). (The mechanism similar to Fig. 2c but with $\alpha < (1/L)$ can be shown to give an inferior solution to the case $\alpha > (1/L)$.) When calculating the energy dissipation rates one can use the symmetry in the velocity fields and need only calculate the energy dissipation rates in hinges AE, AB and (where applicable) EF as well as the plastic work rate involved in the twisting of, say, region I.

Because of the simple geometry most of the terms in eqn (8) are zero for particular hinges since either $\beta = 0$ or $\pi/2$ if η_i are associated with the x and θ directions. We will therefore consider each hinge in turn.

Hinge AB: Let $\dot{\mathcal{D}}_{AB}$ = energy dissipation rate within hinge AB. From eqns (3) and (6) it can be shown that the only non-zero terms in eqn (2) arise from $[\dot{u}]$ and $[\partial \dot{w}/\partial x]$, i.e. the N_x and M_x terms. Again, following Jones and Walters [9], we use the limited interaction yield surface shown in Fig. 3, which, together with the associated normality rule, implies that $|N_x| = N_0 = \sigma_0 t$ and $|M_x| = M_0 = (\sigma_0 t^2/4)$ where σ_0 is the uniaxial yield stress of the material.

Thus

$$\dot{\mathcal{D}}_{AB} = 2\int_0^{\pi/4} \left\{N_x[\dot{u}] + M_x\left[\frac{\partial \dot{w}}{\partial x}\right]\right\} r\,d\theta.$$

Now,

$$[\dot{u}] = 2\alpha r^2 \Omega \left(\frac{\pi}{4} - \theta + \sin\theta - \cos\theta\right)$$

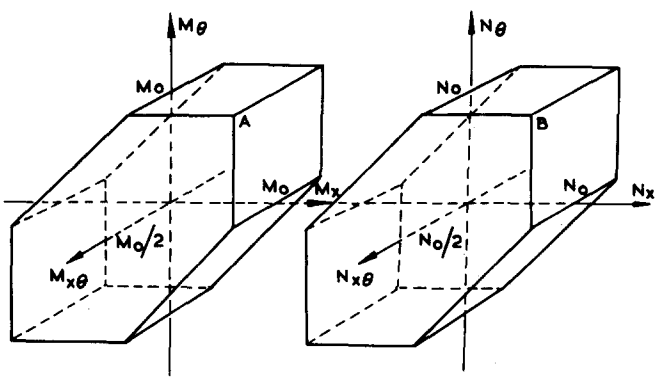

Fig. 3. Limited interaction yield surface.

and

$$\left[\frac{\partial \dot{w}}{\partial x}\right] = 2\alpha r\Omega(\cos\theta - \sin\theta).$$

Since $[\dot{u}] < 0$ and $[\partial \dot{w}/\partial x] > 0$, the normality rule implies that $N_x = -N_0$ and $M_x = M_0$, therefore

$$\dot{\mathcal{D}}_{AB} = 2\int_0^{\pi/4} \left\{2N_0\alpha r^2\Omega\left(\cos\theta - \sin\theta + \theta - \frac{\pi}{4}\right) + 2M_0\alpha r\Omega(\cos\theta - \sin\theta)\right\} r\,d\theta$$

$$= 4\alpha r^2\Omega\left\{N_0 r\left(\sqrt{2} - \frac{1}{2}\left(\frac{\pi}{4}\right)^2 - 1\right) + M_0(\sqrt{2} - 1)\right\}.$$

Let

$$b = \sqrt{2} - \frac{1}{2}\left(\frac{\pi}{4}\right)^2 - 1 = 0.106 \text{ and } c = \sqrt{2} - 1 = 0.414.$$

$$\therefore \dot{\mathcal{D}}_{AB} = 4\alpha r^2\Omega(N_0 rb + M_0 c). \tag{9}$$

Hinge AE: Let $\dot{\mathcal{D}}_{AE}$ = energy dissipation rate within hinge AE. From eqns (3) and (7) it can be shown that the only discontinuity across AE is in $\partial \dot{w}/\partial\theta$. Thus from eqn (2) we have

$$\dot{\mathcal{D}}_{AE} = \int_0^s \frac{M_\theta \left[\frac{\partial \dot{w}}{\partial \theta}\right]}{r} dx$$

where $[\partial \dot{w}/\partial\theta] = 2(1 - \alpha x)r\Omega$, so that

$$\dot{\mathcal{D}}_{AE} = \int_0^s 2M_\theta(1 - \alpha x)\Omega\, dx. \tag{10}$$

If the length of region I is s (i.e. $AE = s$ in Fig. 2a), the rate of dissipation of energy in plastic twisting of the region is given from eqn (1) by

$$\dot{\mathcal{D}}_T = \int_0^s \int_0^{\pi/2} 2M_{x\theta}\,\dot{\kappa}_{x\theta}\, r\,d\theta dx.$$

Using the limited interaction surface and eqn (5) leads to

$$\dot{\mathcal{D}}_T = \frac{\pi}{2} M_0\alpha r\Omega s. \tag{11}$$

Equations (8), (10) and (11) will now be incorporated into the analyses of the collapse mechanisms shown in Figs. (2b–d).

Ring mode (Fig. 2b). In this case $\alpha = 0$ and $s = L$ so that $\dot{\mathcal{D}}_{AB} = \dot{\mathcal{D}}_T = 0$. Since the generalised strain rate associated with M_θ reduces to $2\Omega(>0)$ we have $M_\theta = M_0$, hence

$$\dot{\mathcal{D}}_{AE} = \int_0^L 2M_0\Omega dx = 2M_0\Omega L.$$

Equating the rate of working of the external forces to the rate of energy dissipation in the hinges, we have

$$2Pr\Omega = 8\dot{\mathcal{D}}_{AE} = 16M_0\Omega L$$

$$\therefore P = P_R = \frac{8M_0 L}{r} = \frac{2\sigma_0 t^2 L}{r}. \tag{12}$$

This is of course the usual four hinge mechanism collapse load for a ring subjected to point loads[10] or the initial collapse load of a tube compressed between flat plates[11].

Reversing ovality mode (*Fig.* 2*c*). It can be shown that the only significant mode which involves bending of the generators and in which the whole of the tube deforms is that shown in Fig. 2(c), i.e. with $\alpha > (1/L)$; the ends of the tube ovalise in the reversed sense to the central cross section. Because of this there is a change in the sign of the generalised strain rate corresponding to M_θ and thus we have

$$M_\theta = M_0 \qquad \text{for } 0 \leqslant x < \frac{1}{\alpha}$$

$$M_\theta = -M_0 \qquad \text{for } \frac{1}{\alpha} < x \leqslant L.$$

Equation (1) then becomes

$$\dot{\mathscr{D}}_{AE} = 2M_0\Omega\left\{\int_0^{1/\alpha}(1-\alpha x)\,dx + \int_{1/\alpha}^{L}(\alpha x - 1)\,dx\right\}$$

$$= 2M_0\Omega\left(\frac{1}{\alpha} + \frac{\alpha L^2}{2} - L\right).$$

Equation (11) gives

$$\dot{\mathscr{D}}_T = \frac{\pi}{2} M_0 \alpha r \Omega L.$$

The work rate/energy dissipation rate equation for this mechanism gives

$$2Pr\Omega = 4\dot{\mathscr{D}}_{AB} + 8\dot{\mathscr{D}}_{AE} + 8\dot{\mathscr{D}}_T$$

$$P = 8\sigma_o t r\alpha\left(rb + \frac{tc}{4}\right) + \frac{2\sigma_0 t^2}{r}\left(\frac{1}{\alpha} + \frac{\alpha L^2}{2} - L\right) + \frac{\pi}{2}\sigma_0 t^2 \alpha L$$

$$= \frac{2\sigma_0 t^2}{r\alpha} + \alpha\sigma_0 t^2 r\left(8b\frac{r}{t} + 2c + \frac{\pi L}{2r} + \frac{L^2}{r^2}\right) - \frac{2\sigma_0 t^2 L}{r}. \tag{13}$$

Before proceeding let us examine the coefficient of the α term. Since $b \simeq c/4 \simeq 0.1$ and $r/t \gg 1$, the second term can be neglected compared with the first. it will be clear below that when this mode of collapse occurs the third term is an order of magnitude smaller than the last term in the brackets and can therefore also be neglected. Thus eqn (13) becomes

$$P = \frac{2\sigma_0 t^2}{r\alpha} + \alpha\sigma_0 t^2 r\left(\frac{8br}{t} + \frac{L^2}{r^2}\right) - \frac{2\sigma_0 t^2 L}{r}. \tag{14}$$

It will be shown below that the neglect of the two terms described above provides the key step in establishing the analogy with the beam-foundation problem. The order of magnitude argument is equivalent to saying that the axial bending and panel twisting contributions to the total energy dissipation rates for this mechanism are negligible and that the main interaction is between axial stretching in the central hinge and circumferential bending in the rest of the cylinder. This is very similar to the conditions identified by Calladine in his approximate elastic analysis of the "pinched" cylinder.

Minimising the expression for P with respect to α leads to the optimum value of α, α^*, which is given by

$$\alpha^* = \sqrt{\left(\frac{2t/r}{8br^2 + (tL^2/r)}\right)}. \tag{15}$$

The collapse load, P_O, is therefore

$$P_O = 2\sigma_0 t\sqrt{\left(\frac{2t}{r}\left(8br^2+\frac{tL^2}{r}\right)\right)}-\frac{2\sigma t^2 L}{r}. \tag{16}$$

Localised mode (*Figs. 2a and d*). The analysis of this final mechanism follows in the same way as for the two sets of calculations given above with the following modifications.

(i) Since the half-length of the zone of deformation is s then $\alpha = (1/s)$.

(ii) The deforming region is bounded by generalised hinges (*EFGH* and *E'F'G'H'*) which separate the deforming part from the rigid end regions (V and V'). It can easily be shown that $\dot{\mathcal{D}}_{EF} = (1/2)\ \dot{\mathcal{D}}_{AB}$.

Equating the work rate of the external forces to the energy dissipation rate for this mode gives

$$2Pr\Omega = 4\dot{\mathcal{D}}_{AB} + 8\dot{\mathcal{D}}_{AE} + 8\dot{\mathcal{D}}_{EF} + 8\dot{\mathcal{D}}_{T}.$$

Substituting for the various dissipation rates and once more ignoring the axial bending contribution in $\dot{\mathcal{D}}_{AB}$ gives

$$P = 16\sigma_0\frac{br^2t}{s}+\sigma_0\frac{t^2 s}{r}+\frac{\pi}{2}\sigma_0 t^2. \tag{17}$$

Minimising with respect to s leads to optimum values for $s = s^*$ and $P = P_L$. Thus

$$s^* = 4r\sqrt{\left(\frac{br}{t}\right)}$$

and

$$P_L = 8\sigma_0 t^2\sqrt{\left(\frac{br}{t}\right)}+\frac{\pi}{2}\sigma_0 t^2. \tag{18}$$

For the r/t ratios usually considered, the first term is significantly greater than the second (which arises from the twisting deformation) and this is again ignored to give

$$P_L = 8\sigma_0 t^2\sqrt{\left(\frac{br}{t}\right)}. \tag{19}$$

Ranges of validity

By examining the conditions for which each of the three collapse loads is less than the other two it is easily shown that the various mechanisms are applicable only within certain ranges of tube length. These are summarised below:

$$\begin{aligned} &P_C = P_R \quad \text{for} \quad 0 < L < 2r\sqrt{\left(\frac{2br}{t}\right)} \\ &P_C = P_O \quad \text{for} \quad 2r\sqrt{\left(\frac{2br}{t}\right)} < L < 8r\sqrt{\left(\frac{br}{r}\right)} \\ &P_C = P_L \quad \text{for} \quad L > 8r\sqrt{\left(\frac{br}{t}\right)} \end{aligned} \tag{20}$$

where P_C is the collapse load for the "pinched" cylinder.

ANALOGY WITH RIGID-PLASTIC BEAM-FOUNDATION PROBLEM

Centrally loaded rigid-plastic beam supported by a rigid-plastic Winkler foundation

Consider a rigid-plastic beam of length $2L$ having a yield moment M_p and supported by a rigid-plastic foundation with yield pressure p_0. The calculation of the collapse values of the load P applies at its center as shown in Fig. 4(a) is straightforward and can be considered as a special

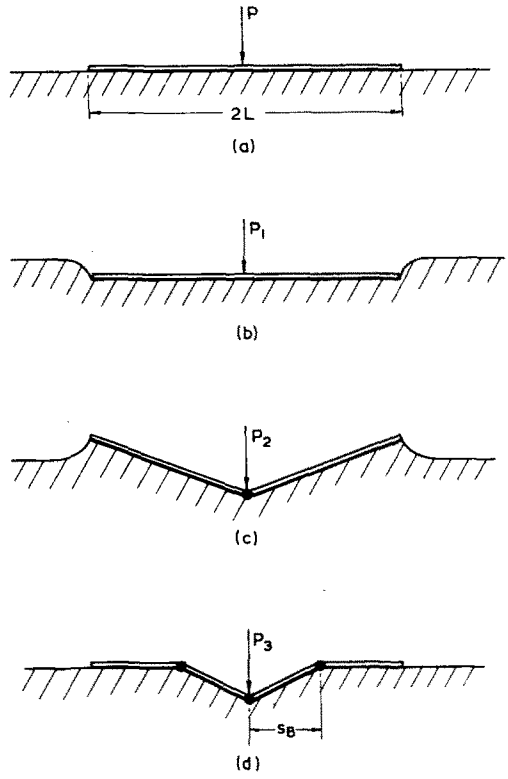

Fig. 4. (a) Rigid-plastic beam on rigid-plastic foundation with a central load, P. (b)–(d) Alternative collapse modes.

case of those problems treated by Boström[12]. Consequently, details of the solution will be omitted. There are three competing collapse modes which are shown in Fig. 4(b–d) and their corresponding collapse loads and ranges of validity are as follows

$$\begin{aligned} P_B &= P_1 = 2p_0L && \text{for} \quad 0 < L < \sqrt{\left(\frac{2M_p}{p_0}\right)} \\ P_B &= P_2 = 2\sqrt{(2p_0(2M_p + p_0L^2))} - 2p_0L && \text{for} \quad \sqrt{\left(\frac{2M_p}{p_0}\right)} < L < 4\sqrt{\left(\frac{M_p}{p_0}\right)} \\ P_B &= P_3 = 4\sqrt{(M_pp_0)} && \text{for} \quad L > 4\sqrt{\left(\frac{M_p}{p_0}\right)}. \end{aligned} \tag{21}$$

For the localised mechanism (Fig. 4d), the optimum value of s_B, s_B^*, is given by

$$s_B^* = 2\sqrt{\left(\frac{M_p}{p_0}\right)}. \tag{22}$$

Rigid-plastic cylindrical shell subjected to a central ring load

As indicated in the introduction, the problem of a rigid-plastic cylindrical shell to which is applied a radial ring load has been examined by a number of authors[1–3]. The solution of the problem posed by an inward ring load of P/unit length applied at the central cross section of a free-ended cylinder (Fig. 5a) is particularly simple when the limited interaction yield surface used earlier is applied and will be included for completeness. For a cylinder of radius R, length $2L$ and wall thickness T, the material having a yield stress σ_0, the solution again consists of three possible collapse modes (ignoring the possibility of circumferential buckling) which are shown in Figs. 5(b–d). Summarising the solution in the same manner as above, the collapse

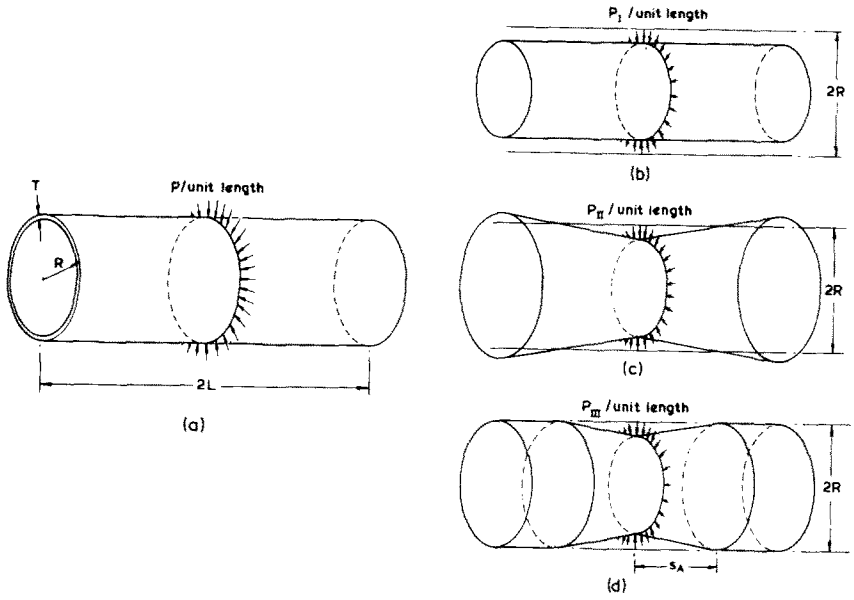

Fig. 5. (a) Rigid-plastic cylinder subjected to ring-load applied at central cross section. (b)–(d) Alternative collapse modes.

values of P, P_A, are given by

$$\begin{aligned} P_A = P_{\mathrm{I}} &= \frac{2\sigma_0 TL}{R} && \text{for} \quad 0 < L < \sqrt{\left(\frac{RT}{2}\right)} \\ P_A = P_{\mathrm{II}} &= \frac{2\sigma_0 T}{R}\sqrt{(RT + 2L^2)} - \frac{2\sigma_0 TL}{R} && \text{for} \quad \sqrt{\left(\frac{RT}{2}\right)} < L < 2\sqrt{(RT)} \\ P_A = P_{\mathrm{III}} &= \frac{2\sigma_0 T}{R}\sqrt{(RT)} && \text{for} \quad L > 2\sqrt{(RT)}. \end{aligned} \tag{23}$$

The optimum value of the half-length of the deformed zone for the localised mode (Fig. 5d), $s_A = s_A{}^*$, is given by

$$s_A{}^* = \sqrt{(RT)}. \tag{24}$$

Beam-foundation analogies

It is clear from eqns (21)–(24) that a formal analogy exists between the solution of the beam-foundation problem and that of the ring-loaded cylindrical shell. This can be expressed as follows

$$\begin{aligned} P_B &\leftrightarrow P_A \\ M_P &\leftrightarrow \frac{\sigma_0 T^2}{4} \\ p_0 &\leftrightarrow \frac{\sigma_0 T}{R}. \end{aligned} \tag{25}$$

Similarly the approximate solution for the "pinched" cylinder as expressed by eqns (20) can also be associated with the solution of the beam-foundation problem through the relationships

$$\begin{aligned} P_B &\leftrightarrow P_C \\ M_P &\leftrightarrow 4b\sigma_0 r^2 t \\ p_0 &\leftrightarrow \frac{\sigma_0 t^2}{r}. \end{aligned} \tag{26}$$

Discussion of the beam-foundation analogies

The solutions of the three problems given above constitute the simplest of their type principally because of the particular yield surface used to represent the behaviour of the shell. However, whilst more exact yield surfaces modify the details of the solution (and certainly increase the complexity of the calculations) the qualitative features of the solutions remain the same vis à vis the number of different collapse mechanisms and the parametric groups that appear in the solutions.

Having established the basis of the analogy between the rigid-plastic beam-foundation system and the two rigid-plastic cylindrical shell problems one can, within limits, translate the solution of a specific beam-foundation problem into that for equivalent shell problems. Conversely, one can seek the solution of a given shell problem from a catalogue of solutions of beam-foundation problems. Since rigid-plastic beam-foundation problems are relatively simple to solve one can easily produce such a catalogue. Furthermore, the paper by Boström[12] already supplies a useful set of solutions.

This procedure cannot be adopted without justification for all beam-foundation problems. In particular, if one considers a fixed-ended beam, its response changes due to the influence of axial forces as the deflection increases[13]. This effect depends upon the nature of the interaction between the bending moment and axial force within the beam. Whilst similar effects would be expected in fixed-ended cylindrical shells their deduction from an "equivalent" beam-foundation problem would require further investigation. Similar caution needs to be exercised when considering other secondary effects in the post-limit load state such as those due to strain-hardening.

However, within these limitations, one can establish formal solutions to a whole range of shell problems in which the loading consists of opposed radial loads applied across a diameter involving free, position-fixed or built-in end conditions or combinations thereof. These solutions should only be considered to be formal ones and their usefulness and relevance needs to be assessed. With regard to the axisymmetric loading problem the usefulness of the limit analysis solutions is already well established and such solutions are frequently used as an aid to the design of various components of pressure vessels (see for example Refs. [4] and [14]) and so they will not be discussed further.

The main topic of interest in this paper is the solution of non-axisymmetric problems as exemplified by the "pinched" cylinder problem and here the usefulness of the solution is less clear. As explained in the Introduction, interest in this problem stems from the large deflection behaviour of tubes crushed by opposed indenters and as such the solution above can be considered to be a preliminary attempt to provide a suitable theoretical model. This is discussed more fully in the next section in which a comparison is made with the results of a series of experiments which have been published recently.

The solution given above is the rigid-plastic equivalent of the elastic solution presented by Calladine[6] and possesses many of the same features as this solution with regard to the basis of the beam-foundation analogy and the characteristic length scale, $r\sqrt{(r/t)}$, which appears in the solution. This would seem to imply the possibility of "long wavelength" behaviour in rigid-plastic non-axisymmetric loading problems compared with the "short wavelength" (length scale $\sqrt{(rt)}$) response to axisymmetric loading, again in broad agreement with the corresponding elastic behaviour. Also Calladine discusses the "pinched" cylinder by analysing individual Fourier components of the displacement field and in a similar manner one could analyse the deformation of a rigid-plastic tube subjected to a series of radial loads equally spaced around a given circumference. Presumably one would find that, for long tubes, the deformed length reduced as the number of applied loads was increased in a manner similar to that in the solution for higher order Fourier components.

COMPARISON BETWEEN "PINCHED" CYLINDER SOLUTION AND EXPERIMENTS ON THE CRUSHING OF TUBES

Very few attempts have been made to examine the plastic response of locally loaded metal cylinders. Morris and Calladine[15] analysed the behaviour of a cylindrical shell when loaded radially through a pair of circular bosses principally to examine the stability of the deformation when account was taken of changes in geometry. For radial deflections of the order of a few

thicknesses, the deformation was localised in the vicinity of the boss and they were able to follow the deformation by postulating a sequence of kinematically admissible velocity fields and performing corresponding upper bound calculatons. In these the shell was treated as a three-dimensional body. It is clear that the deformation involved bending and membrane action although it was found to be easier not to separate these two effects in the manner usually employed for shell problems. Their main interest was in shells having r/t ratios of the order of 50.

The work which motivated the approach described above was that described in [7] which was concerned with the large deformation of circular tubes produced by opposed wedge-shaped indenters. The central cross section of the tube was severely ovalised and hence was subjected, at least qualitatively, to the type of mode of deformation used in the analysis. The main features of this work will be summarised below and reference will be made to the change in the nature of the post-yield behaviour as the tube length is increased.

Large plastic deformation of tubes by opposed wedge shaped indenters

Watson *et al.*[7] recently described a series of experiments in which circular metal tubes were crushed by a pair of oppposed wedge-shaped indenters applied at the central cross section of the tube. It was found that, as the tube length was increased, four different modes of behaviour were observed, these were

(i) Ring Mode (Fig. 6), for short tubes, $2L < 1.5D$. In this mode the generators of the tube remained essentially straight and the tube deformed almost as if compressed between flat plates extending over the whole length of the tube.

(ii) A Transitional Mode (Fig. 7), for medium length tubes, $1.5D < 2L < 5D$. The tubes began by deforming in a pseudo-ring in which the vertical end diameters reduce with the correspponding dimension at the central cross section although at a slower rate. This phase stops at a certain stage in the deformation after which the vertical diameter begins to increase and continues to do so for the remainder of the duration of loading (see Fig. 7a).

(iii) A Reversing Ovality Mode (Fig. 8), for tubes for which $2L > 5D$. These tubes are such that the vertical end diameters increase from the beginning of the loading so that the sense of the ovalisation caused at the ends is opposite to that caused in the vicinity of the central cross section by the indenters.

(iv) The amount of end ovalisation reduces as the length of the tube increases and for $2L > 8D$ approximately there is little increase in the load carrying capacity of the tube. As noted in [7], when reversing ovality occurs, the deformation within the wall of the tube appears to be almost inextensional for the shorter tubes whereas for the long tubes the mode of deformation shows significant axial stretching. This latter behaviour is coupled with the fact that the deformation appears to be limited to only certain portions of the tube either side of the indenter. Outside these portions the deformation is slight and these parts of the tube do not contribute to the load carrying capacity as already noted.

A gradual change in the character of the load-deflection graphs is also clear from Figs. 6–8. The behaviour ranges from a limit load type of response reminiscent of tubes compressed between flat plates to a response in which it is difficult to detect a collapse load as such and which might be termed "degenerate" in the sense defined by Demir and Drucker[16]. They state that "limit loads are known to be excellent measures of load carrying capacity for ductile structures or structural elements when two conditions are met. The first is that excessive deformations or deflections occur before the influence of strain-hardening becomes appreciable. The second is that the alteration in the geometry of the structure produced by the deflection has but a negligible effect on the load required to continue deformation". They reserve the term "degenerate" for cases in which geometry changes *do* have a significant effect in increasing the load. This occurs principally in situations in which the collapse mode involves bending deformations which in turn lead to the development of membrane stresses causing a rapid stiffening of the structural response as exemplified by a clamped plate[17] or beam[13]. For long tubes there is certainly an element of degeneracy in this sense. It would seem that both of the phenomena mentioned by Demir and Drucker, strain hardening and geometry change, play a part in the large deflection response of centrally loaded tubes. The stiffening of the short tubes as the deflection increases is similar to that of a tube compressed between flat plates. Recently Reid

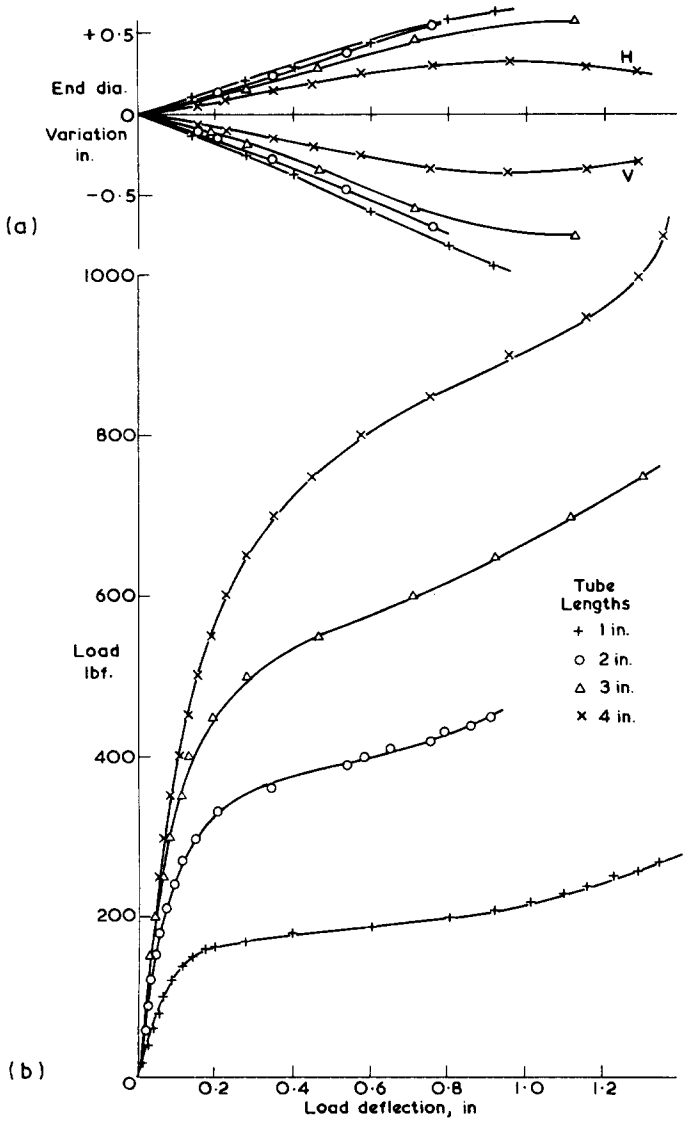

Fig. 6. Characteristics of short aluminium tubes (ring mode). ($r = 1$ in., $t = 0.064$ in.). (a) Variation of end diameters with load-deflection. (b) Load vs load-deflection.

and Reddy[18] have re-examined this problem and have shown that the increase in the load required to continue the deformation can be attributed in the main to the influence of strain hardening. However, these shorter tubes do display a clear limit load and strain hardening only has a significant effect at deflections in excess of $\delta/D = 0.3$, say.

In summary, therefore, the problem examined by Watson *et al.*[7] is a most complicated one to analyse fully. An attempt was made however, to produce a quantitative assessment of the load-deflection behaviour of the reversing ovality tubes up to $\delta/D = 0.6$ by performing an upper bound calculation based upon the mode of deformation suggested by the experiments. This neglected the effects of strain hardening and produced reasonable agreement with the experimental data which would seem to imply that the degeneracy effect (i.e. the bending-membrane stretching interaction) perhaps predominates in this deflection range.

Comparison with "pinched" cylinder solution

The limit analysis solution described above is characterised by the fact that the whole of the central cross section of the tube is involved in the deformation mode. For short tubes which have a reasonably well defined limit load this assumption is reasonable and the collapse load is adequately estimated by eqn (12). Using the relevant yield stress (which is 35,000 lbf/in.^{2}), eqn

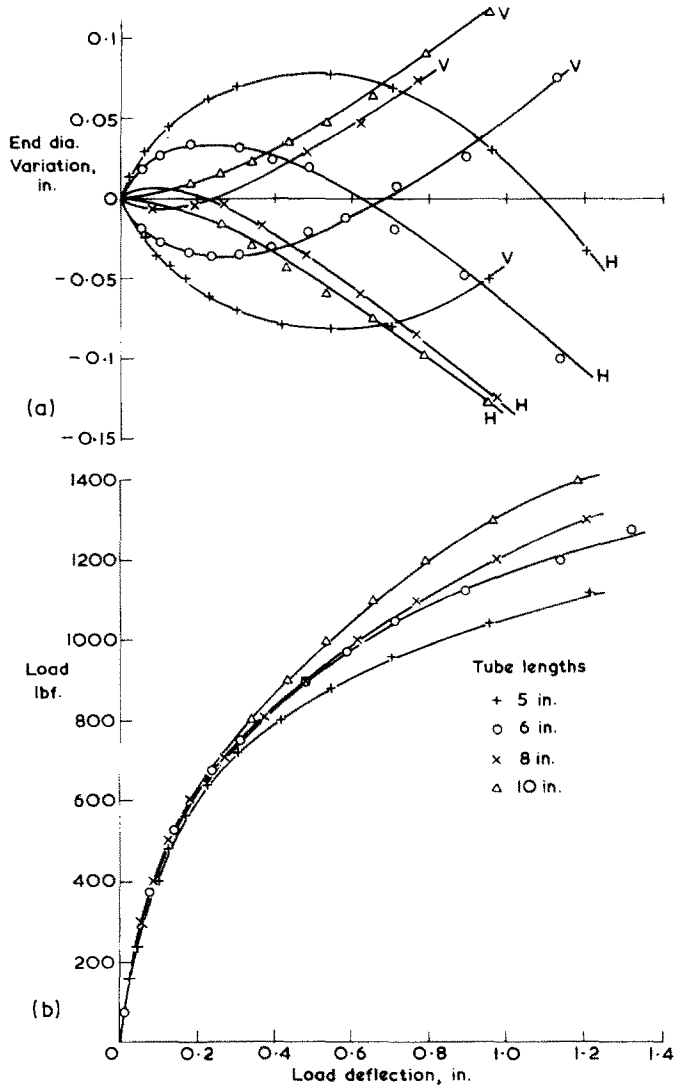

Fig. 7. Characteristics of medium length aluminium tubes (reversing ovality). ($r = 1$ in., $t = 0.064$ in.). (a) Variation of end diameters with load-deflection. (b) Load vs load-deflection.

(12) gives a limit load of 143 lbf/in. of tube length. As the tube length is increased the problem becomes increasingly degenerate and one feature of this is that the first departure of the load-deflection curves from linearity becomes independent of the tube length (unlike Fig. 6b) and is governed by local deformation around the indenters similar to that examined by Morris and Calladine[16]. Thus the onset of nonlinearity occurs in Figs. 7(b) and 8(b) at around 400–450 lbf. The collapse loads given by eqns (16) and (19), being based on a collapse mechanism which differs significantly from the localised collapse mechanism observed experimentally, therefore, only constitute fairly crude upper bounds. (They give values of 1,050 lbf and 1,476 lbf respectively.) However, as the deformation proceeds the whole of the central cross section does participate in the ovalisation and this ovalisation "propagates" down the tube so that cross sections over a finite region of the tube are also affected.

It is therefore likely that, whilst the "pinched" cylinder analysis inadequately predicts the initial limit load, its predictions regarding the influence of the geometrical parameters on the extent of the deformed region and on the changes in deformation mode may be significant. The tubes whose behaviour is described in Figs. 6–8 were made of aluminium and had a 2 in. outside dia. and a nominal wall thickness of 0.064 in. Since the Transitional Mode begins as a Ring Mode it seems reasonable to combine the two length ranges indicated for the purpose of comparison with the incipient collapse analysis given earlier. Thus Ring-type behaviour can be

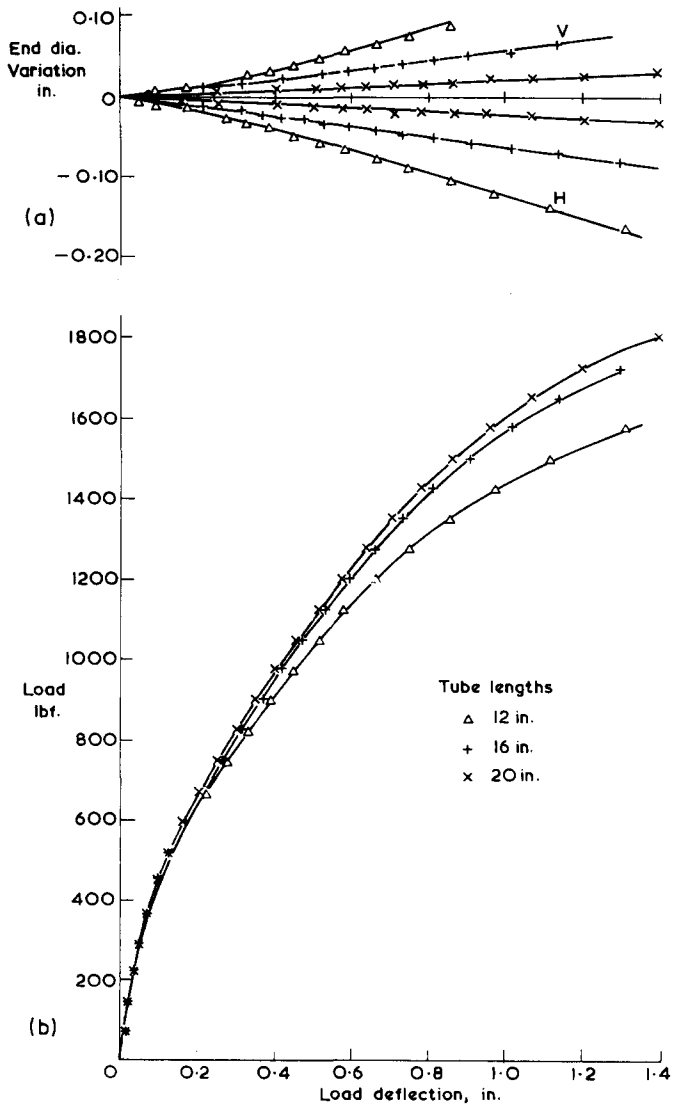

Fig. 8. Characteristics of long aluminium tubes (localised mode). ($r = 1$ in., $t = 0.064$ in.). (a) Variation of end diameters with load-deflection. (b) Load vs load-deflection.

considered to have ceased when 2L is greater than 4 or 5D. Regarding the switch to the localised mode of deformation we can assess the minimum length of tube beyond which additional tube length has minimal effect on the load carrying capacity of the tube from Fig. 8(b). This indicates that little change occurs when the length exceeds 8 or 9D. Equation (20i) predicts that a switch from Ring Mode to Reversed Ovality occurs at $L = 2r\sqrt{(2br/t)} = D\sqrt{(2br/t)}$. Using $r = 1$ in., $t = 0.064$ in. and $b = 0.10$ in. gives $2L = 3.6D$. Equation (20iii) indicates that the change to the localised deformation mode occurs at $L = 8r\sqrt{(br/t)} = 4D\sqrt{(br/t)}$, i.e. 2L = 10D. Both of these estimates are therefore in reasonable agreement with the observations from the experiments.

CONCLUSIONS

An upper bound solution for the problem of a "pinched" free-ended circular cylinder has been presented which incorporates the effects of cross-sectional ovalisation as opposed to local plastic collapse. By comparing this solution with the solution of an equivalent rigid-plastic beam-foundation problem a simple analogy is established between them by which the formal solutions of a range of similar shell problems can readily be produced.

In order to examine the limitations of the solution a comparison is made with the behaviour of aluminium tubes centrally loaded by opposed indenters. Whilst the limit loads are shown to

be rather crude estimates of the levels at which plastic effects first become dominant in the tube response, the roles of the various geometrical parameters in affecting changes in deformation mode are predicted with reasonable accuracy. It is clear that if a theoretical model is required for the small deformation plastic behaviour of locally loaded metal tubes, a method such as that described by Morris and Calladine[16] should be used which can cope with the onset of degeneracy and follow its development.

Acknowledgement—The author would like to express his gratitude to Mr. C. R. Calladine and Mr. T. Yella Reddy for useful discussions during the preparation of this paper.

REFERENCES

1. D. C. Drucker, Limit Analysis of Cylindrical Shells under Axially Symmetric loading. *Proc. 1st Midwest. Conf. Solid Mech.*, Urbana, Illinois, 158–163 (1953).
2. G. Eason and R. T. Shield, The influence of free ends on the load carrying capacities of cylindrical shells. *J. Mech. Phys. Solids* **4**, 17–27 (1955).
3. G. Eason, The load carrying capacities of cylindrical shells subjected to a ring of force. *J. Mech. Phys. Solids* **7**, 169–181 (1959).
4. K. S. Dinno and S. S. Gill, The limit analysis of a pressure vessel consisting of the junction of a cylindrical and spherical shell. *Int. J. Mech. Sci.* **7**, 21–42 (1965).
5. J. P. Den Hartog, *Advanced Strength of Materials*. McGraw-Hill, New York (1952).
6. C. R. Calladine, Thin-walled elastic shells analysed by a Rayleigh Method. *Int. J. Solids Structures* **13**, 515–530 (1977).
7. A. R. Watson, S. R. Reid, W. Johnson and S. G. Thomas, Large deformations of thin-walled circular tubes under transverse loading—II. *Int. J. Mech. Sci.* **18**, 387–397 (1976).
8. W. Johnson and S. R. Reid, Metallic energy absorbing systems. *Appl. Mech. Rev.* **31**(3), 277–288 (1978).
9. N. Jones and R. M. Walters, A comparison of theory and experiments on the dynamic plastic behaviour of shells. *Arch. Mech. (Arch. Mech. Stos.)* **24**, 701–714 (1972).
10. C. Huang, Plastic collapse of thin rings. *J. Aero. Sci.* **20**, 819–824 (1953).
11. J. A. De Runtz and P. G. Hodge, Crushing of a tube between rigid plates. *J. Appl. Mech.* **30**, 391–395 (1963).
12. P. O. Boström, Collapse modes of a rigid-beam on a rigid-plastic foundation. *Int. J. Mech. Sci.* **17**, 73–84 (1975).
13. S. S. Gill, Effect of deflexion on the plastic collapse of beams with distributed load. *Int. J. Mech. Sci.* **15**, 465–471 (1973).
14. H. McIntyre, J. N. Ashton and S. S. Gill, Limit analysis of a pad reinforced flush nozzle in a spherical pressure vessel. *Int. J. Mech. Sci.* **19**, 399–412 (1977).
15. A. J. Morris and C. R. Calladine, Simple upper-bound calculations for indentations of cylindrical shells. *Int. J. Mech. Sci.* **13**, 331–344 (1971).
16. H. H. Demir and D. C. Drucker, An experimental study of cylindrical shells under ring loading. *Prog. Appl. Mech., Prager Anniv. Vol.*, 205–220 (1963).
17. E. T. Onat and R. M. Haythornthwaite, The load-carrying capacity of circular plates at large deflection. *J. Appl. Mech.* **23**, 49–55 (1956).
18. S. R. Reid and T. Yella Reddy, Effects of strain-hardening on the lateral compression of tubes between rigid plates. *Int. J. Solids Structures* **14**, 213–225 (1978).
19. S. P. Timoshenko and S. Woinowsky-Krieger, *Theory of Plates and Shells*, 2nd Edn. McGraw-Hill, New York (1959).

APPENDIX

If one considers a ring of radius r subjected to a pair of opposed point loads, it has been shown[10,11] that a suitable initial collapse mode is the four-hinge mode shown in Fig. 9. Considering the quadrant $0 < \theta < (\pi/2)$, its incipient motion is one of rotation about the instantaneous centre C. The radial and tangential velocity components of a typical point Q are

$$\dot{w} = -x_Q\Omega \text{ and } \dot{v} = y_Q\Omega$$

where x_Q and y_Q are the lengths shown in Fig. 9 and Ω is the angular velocity of the quadrant in the incipient deformation mode. Simple geometry leads to

$$x_Q = r(\cos\theta - \sin\theta) \text{ and } y_Q = r(\sin\theta + \cos\theta - 1).$$

Thus

$$\dot{w} = r\Omega(\sin\theta - \cos\theta) \tag{A1}$$

$$\dot{v} = r\Omega(\sin\theta + \cos\theta - 1). \tag{A2}$$

These equations describe the basic ovalising velocity field for a ring and since the mode of deformation of the "pinched" cylinder is one in which each cross-section ovalises, they will be taken as the basis for describing the velocity field of segments of the cylinder.

Let us assume that the mode of deformation is a simple extension of that for a tube compressed between flat plates and consists of four cylindrical panels in each half of the cylinder as shown in Fig. 2(a). Furthermore, let us assume that the mid-surface of the panels is inextensional except possibly across generalised hinges separating the various sectors of the cylinder. The conditions of inextensibility are[19]

$$\frac{\partial \dot{u}}{\partial x} = 0 \tag{A3}$$

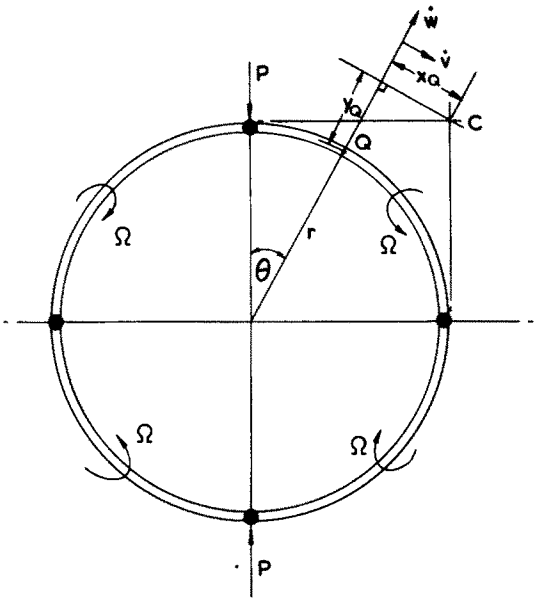

Fig. 9. Collapse mechanism for a ring (tube) under opposed point (line) loads.

$$\frac{1}{r}\frac{\partial \dot{v}}{\partial \theta}+\frac{\dot{w}}{r}=0 \tag{A4}$$

$$\frac{1}{r}\frac{\partial \dot{u}}{\partial \theta}+\frac{\partial \dot{v}}{\partial x}=0. \tag{A5}$$

In general, these lead to

$$\dot{u}=f(\theta),\quad \dot{v}=(p+qx)g(\theta) \text{ and } \dot{w}=-(p+qx)g'(\theta) \tag{A6}$$

where f is an arbitrary function of θ which is related to g through eqn (A5). From (A1) and (A2) clearly in this case

$$g(\theta)=\sin\theta+\cos\theta-1.$$

Also if the radial velocity at A (Fig. 2) is $-r\Omega$ then we have $p=r\Omega$. Allowing for the magnitude of the radial velocity to reduce away from the load we put $q=-\alpha r\Omega$, where α is the normalised slope of the top generator and conclude that

$$\dot{w}=-(1-\alpha x)r\Omega(\sin\theta-\cos\theta) \tag{A7}$$

$$\dot{v}=(1-\alpha x)r\Omega(\sin\theta+\cos\theta-1) \tag{A8}$$

describe the radial and tangential components of such a mechanism.

From (A5) we have

$$f'(\theta)=\alpha r^2\Omega(\sin\theta+\cos\theta-1)$$

$$\text{i.e. } f(\theta)=\alpha r^2\Omega(\sin\theta-\cos\theta-\theta+K)$$

where K is a constant of integration. For convenience we stipulate that $\dot{u}=0$ at $\theta=(\pi/4)$ which leads to

$$\dot{u}=f(\theta)=\alpha r^2\left(\frac{\pi}{4}-\theta+\sin\theta-\cos\theta\right). \tag{A9}$$

Equations (A7)–(A9) therefore provide a velocity field for the octant $0\leq\theta\leq(\pi/2)$, $x\geq 0$ of a "pinched" cylinder which incorporates the effects of cross-sectional ovalisation.